

## Target waves in the complex Ginzburg-Landau equation

Matthew Hendrey, Keeyeol Nam, Parvez Guzdar,\* and Edward Ott†  
*University of Maryland, Institute for Plasma Research, College Park, Maryland 20742*  
 (Received 28 March 2000)

We introduce a spatially localized inhomogeneity into the two-dimensional complex Ginzburg-Landau equation. We observe that this can produce two types of target wave patterns: stationary and breathing. In both cases, far from the target center, the field variables correspond to an outward propagating periodic traveling wave. In the breathing case, however, the region in the vicinity of the target center experiences a periodic temporal modulation at a frequency, in addition to that of the wave frequency of the faraway outward waves. Thus at a fixed point near the target, the breathing case yields a quasiperiodic time variation of the field. We investigate the transition between stationary and breathing targets, and note the existence of hysteresis. We also discuss the competition between the two types of target waves and spiral waves.

PACS number(s): 82.40.Ck, 47.32.Cc, 47.54.+r

### I. INTRODUCTION

Numerous systems have been studied that are capable of spontaneously producing spatiotemporal patterns. In experiments, two of the most common patterns seen are spiral waves and target waves. Spiral waves are spirals that steadily rotate in time, while target waves consist of concentric circular waves that radiate radially outward from a source. Spiral waves appear in chemical reaction-diffusion systems such as those involving the Belousov-Zhabotinsky reaction [1] and catalytic reactions on surfaces [2]. In biology, slime mold colonies of *Dictyostelium* also produce spiral waves [3,4]. Spiral waves of the electric signal in the heart occur at the onset of ventricular fibrillation [5]. Spiral waves also occur in planar dc driven semiconductor-gas discharge systems [6]. Many of these same systems also exhibit target waves. For example, the Belousov-Zhabotinsky reaction supports target waves [7–9], as do colonies of *Dictyostelium* [4]. In these systems the existence of target waves is often (but not always) attributed to the presence of local inhomogeneities, for example a grain of dust or other impurity [8,10]. For the Belousov-Zhabotinsky reaction, the number of target wave centers decreases when the chemical solution is run through finer filters [8]. In an experiment by Petrov *et al.*, target waves are produced in the light-sensitive Belousov-Zhabotinsky reaction by illuminating a subregion of the system with a light source [11]. Theoretically, Hagan and others stated that target wave solutions are stabilized when a localized inhomogeneity is present [12]. In these works, target waves were studied in reaction-diffusion equations. Many researchers studied spiral waves in oscillatory media by means of the complex Ginzburg-Landau equation (CGLE), which is a generic equation describing spatially extended systems in the vicinity of a Hopf bifurcation [13]. Previous research produced target solutions due to boundary effects [14]. In order to produce target waves in a CGLE descrip-

tion, we introduce a suitable localized inhomogeneity. We find two different types of target wave solutions. The first is a stationary target wave where the field variables vary periodically at the frequency of the emitted outward propagating waves. The second is a breathing target where, in addition to the frequency of the outward propagating waves, there is an additional superimposed temporal modulation at another frequency. We investigate the transition between these two target wave types, and note the existence of hysteresis. We also discuss the pattern competition between the two types of target waves and spiral waves.

The homogeneous complex Ginzburg-Landau equation

$$\frac{\partial A}{\partial t} = \mu A - (1 + i\alpha)|A|^2 A + (1 + i\beta)\nabla^2 A, \quad (1)$$

with  $\mu$  (complex),  $\alpha$  (real), and  $\beta$  (real) constants, describes extended media in which the homogeneous state is oscillatory and near a Hopf bifurcation [13]. The real part of the parameter  $\mu$  measures the deviation from the bifurcation point. The real part of  $\mu$  gives the exponential growth rate of homogeneous perturbations from the  $A=0$  state, and the imaginary part of  $\mu$  is a frequency shift. Typically  $\mu$  is scaled to unity by the following transformations  $A \rightarrow \sqrt{\text{Re}(\mu)} A e^{i\text{Im}(\mu)t}$ ,  $\mathbf{r} \rightarrow \mathbf{r}/\sqrt{\text{Re}(\mu)}$ , and  $t \rightarrow t/\sqrt{\text{Re}(\mu)}$ . A steadily rotating spiral solution to Eq. (1) with  $\mu=1$  has the general form [15]

$$A(\mathbf{r}, t) = F(r) \exp\{i[\sigma\theta + \psi(r) - \omega t]\}. \quad (2)$$

The quantity  $\sigma$  is a positive or negative integer, and is called the topological charge of the spiral. There is a  $2\pi\sigma$  phase change of  $A$  for a counterclockwise path around the spiral center ( $r=0$ ). Stable spiral solutions exist for appropriate  $\alpha$  and  $\beta$  and  $\sigma = \pm 1$  corresponding to a single-armed spiral. In order that the solution remain continuous and finite at  $r=0$ , it is required that  $A(\mathbf{r}=0, t) = 0$ . For small  $r$  the real functions  $F(r) \equiv |A|$  and  $\psi(r)$  behave as  $F(r) \sim r$  and  $d\psi(r)/dr \sim r$ . For large  $r$  the spiral wave asymptotes to a plane wave with wave number  $k$  independent of  $r$ ,

\*Author to whom correspondence should be addressed. Electronic address: guzdar@ipr.umd.edu

†Also at the Department of Physics and Department of Electrical Engineering, University of Maryland.

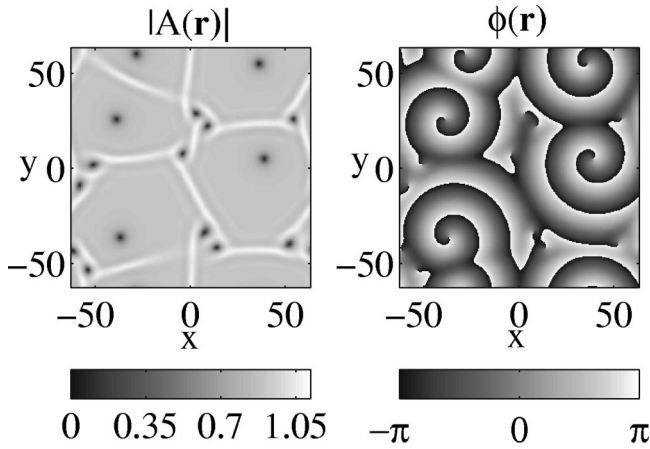


FIG. 1. The magnitude  $|A(\mathbf{r})|$  and phase  $\phi(\mathbf{r})$  of a solution to the homogeneous CGLE [Eq. (1)] with  $\mu=1$ ,  $\alpha=0.34$ , and  $\beta=-1.45$  in the quasifrozen parameter regime. After a transient time the solution has settled down to a very slowly evolving state where the vortices and domain walls remain essentially stationary.

$k = d\psi/dr|_{r \rightarrow \infty}$ . Substituting a constant amplitude plane wave solution,  $A \sim \exp(ikr - i\omega t)$ , into Eq. (1), with  $\mu=1$ , yields the dispersion relation

$$\omega = \alpha + (\beta - \alpha)k^2, \quad (3)$$

and the boundary conditions that, as  $r \rightarrow \infty$ ,  $F(r) \rightarrow \sqrt{1 - k^2}$  and  $d\psi(r)/dr \rightarrow k$ .

In  $(\alpha, \beta)$  space several different regions of solutions of Eq. (1) exist. One such region is the quasifrozen regime where spiral solutions are stable [16]. In this regime spirals form from perturbations of  $A=0$ , and evolve to a quasifrozen state in which many spirals form, each within their own domain [see Fig. 1 which shows a quasifrozen solution obtained at late time from a two-dimensional (2D) numerical solution of Eq. (1) with periodic boundary conditions]. A spiral's domain is the region in space occupied by a spiral's waves. Spiral domains are separated by narrow domain walls, easily seen in the plot of  $|A|$  of Fig. 1. The spiral centers are seen as the dark spots in the  $|A|$  plot or as the center of spiral waves in the phase plot of Fig. 1. The interior of each domain is well approximated by Eq. (2). After a

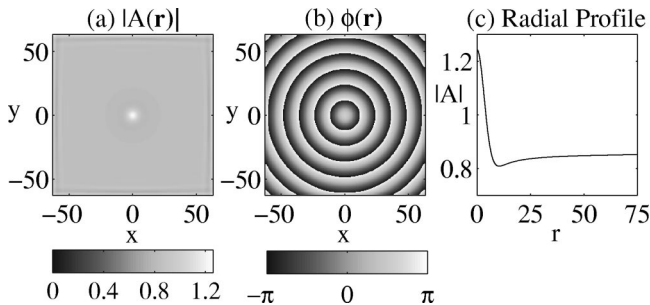


FIG. 2. Stationary target wave for  $\alpha=0.34$ ,  $\beta=-1.45$ ,  $\nu=1$ ,  $\delta=0.82$ , and  $r_o=4$ . The system starts with random initial conditions, and a stationary target dominates after a transient time. (a) The magnitude  $|A(\mathbf{r})|$  does not go to zero at the center as it does for a spiral wave, but increases at the origin due to the larger value of  $Re(\mu)$  at  $r=0$ . (b) Phase  $\phi(\mathbf{r})$ . (c) Radial profile obtained from the 1D radial equation [Eq. (6)]. This profile is stationary in time.

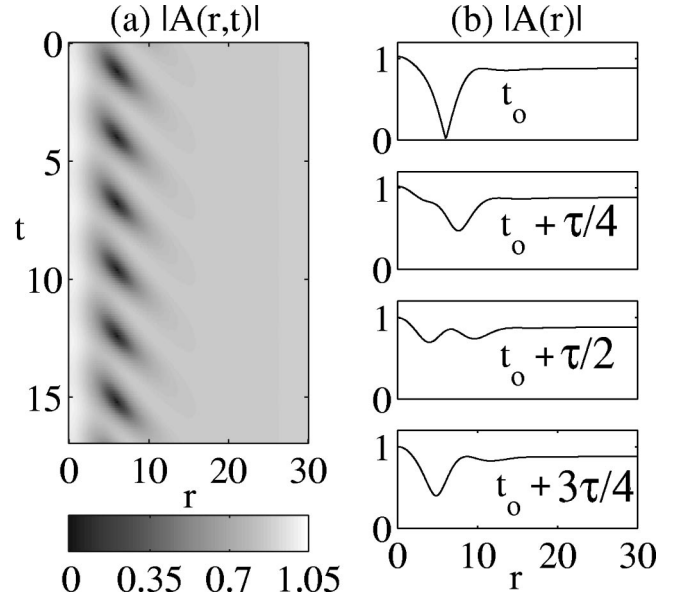


FIG. 3. (a) The magnitude  $|A(r,t)|$  is colorcoded as a function of time and radial distance for the breathing target wave solution. The periodicity of the breathing target is easily visible. This figure is obtained using the one-dimensional code with uniform initial conditions evolved for 1000 time units. (b) Radial profile for  $|A|$  at times  $t_o$ ,  $t_o + \tau/4$ ,  $t_o + \tau/2$ , and  $t_o + 3\tau/4$ , where  $t_o=1.2$  and  $\tau=2.8$ .

transient, the large domains become almost stationary in time; i.e., both the domain walls and the locations of their spiral center evolve very slowly [17].

## II. TARGET WAVES

As we shall see, target wave patterns for the complex Ginzburg-Landau equation result from localized inhomogeneities. We represent a localized inhomogeneity in the complex Ginzburg-Landau equation by making  $\mu$  vary with space [18]. We introduce inhomogeneity in both the real and imaginary parts of  $\mu$ . This corresponds to a spatially varying exponential growth rate and frequency shift, respectively. In particular, we consider the complex Ginzburg-Landau equation

$$\frac{\partial A}{\partial t} = \mu(r)A - (1 + i\alpha)|A|^2A + (1 + i\beta)\nabla^2 A, \quad (4)$$

$$\mu(r) = 1 + (\nu + i\delta)\exp\left[-\left(\frac{r}{r_o}\right)^2\right], \quad (5)$$

where  $\mu(r)$  is axially symmetric, and  $\alpha$ ,  $\beta$ ,  $\nu$ ,  $\delta$ , and  $r_o$  are real constants. Because of the large parameter space we restrict our attention to how  $\delta$  affects the system behavior. Two of our main findings are that in the quasifrozen region of  $(\alpha, \beta)$  space two different types of target waves are seen, and that the transition between the two types of target waves is hysteretic.

Target waves do not have a phase singularity at their center, as do spiral waves. A target wave can be thought of as having a topological charge  $\sigma=0$ ; i.e., no  $\theta$  dependence. One of the two types of target wave solutions that we find

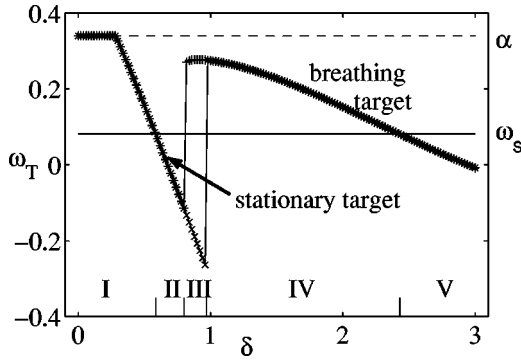


FIG. 4. Target wave frequency  $\omega_T$  as a function of the parameter  $\delta$  from solution of the 1D CGLE [Eq. (6)]. The spiral wave frequency  $\omega_s$  is also plotted where  $\omega_s = 0.08145$ . For  $\delta < 0.3$  the system undergoes bulk oscillation at the frequency  $\alpha = 0.34$ . For  $0.3 < \delta < 0.8$ , the solution goes to a stationary target wave whose frequency is apparently linearly related to  $\delta$ . There is an overlap region of hysteresis for  $0.8 < \delta < 0.97$ . For  $\delta > 0.97$  the system goes to the breathing target wave solution. When 2D numerical solutions of the CGLE [Eqs. (4) and (5)] are evolved from random initial conditions, there are five different regions of behavior observed. Region I produces spiral waves. Region II produces a stationary target wave. Region III produces either spiral waves or a stationary target wave depending on the value of  $\delta$  and the initial conditions. Region IV produces spiral waves. Region V produces a breathing target wave.

has  $|A|$  constant in time; in particular, this target solution is of the form  $A = F_T(r) \exp[i\psi_T(r) - i\omega_T t]$  (where the subscript  $T$  is to distinguish target waves). We call this solution a stationary target wave (though waves do propagate outward). Figure 2 shows a numerical stationary target solution at the parameter values  $\alpha = 0.34$ ,  $\beta = -1.45$ ,  $\nu = 1.0$ ,  $\delta = 0.82$ , and  $r_o = 4.0$ . For these parameters  $\text{Re}(\mu) = 2$  at the origin ( $r = 0$ ), compared with its faraway value of  $\text{Re}(\mu) \rightarrow 1$  as  $r \rightarrow \infty$ . Far away from the origin  $|A|$  approaches its

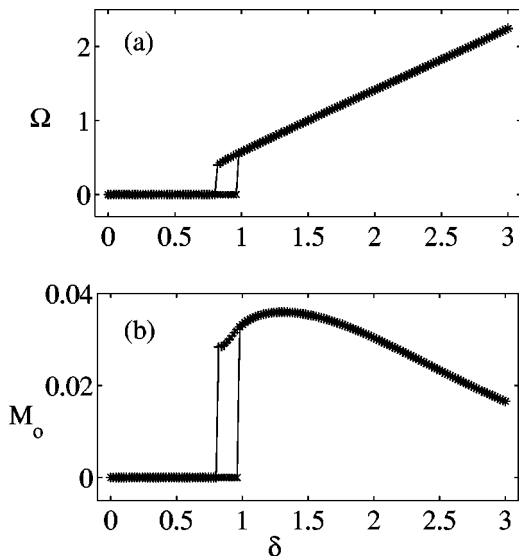


FIG. 5. (a) Frequency of the breathing target wave oscillation  $\Omega$ . (b) Amplitude of the breathing target wave oscillation measured at the origin  $M_o$ . There is a finite jump in both the frequency and amplitude of the breathing oscillation.

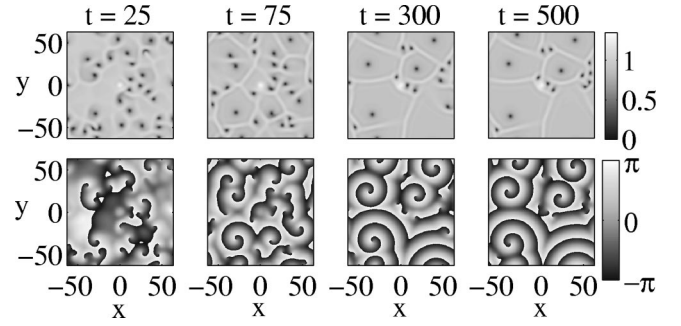


FIG. 6. Time evolution of both the magnitude (top) and phase (bottom) of  $A$  for  $\delta = 0.5$  showing spiral wave domination over the stationary target wave. This corresponds to region I in Fig. 4.

asymptotic value of  $\sqrt{1 - k^2}$ , where  $k$  is the wave number of the outward propagating target wave. For large  $r$  the equation becomes a homogeneous CGLE, and the target wave solution approaches a plane wave solution with a dispersion relation given by Eq. (3). The breathing target waves have magnitudes that oscillate sinusoidally in time in the region of the inhomogeneity. Figure 3(a) shows  $|A|$  as a function of  $r$  and  $t$  for the same parameter values of  $\alpha$ ,  $\beta$ ,  $\nu$ , and  $r_o$  as in Fig. 2, but now with  $\delta$  increased to  $\delta = 3$ . Figure 3(b) shows the radial profile of  $|A|$  at several different times. We characterize the breathing target by measuring the frequency  $\Omega = 2\pi/\tau$  and amplitude  $M_o$  of the oscillation of  $|A|$  at the origin.

In order to understand the relationship between the stationary and breathing targets, we numerically determine the frequency  $\omega_T$  of the outward propagating target waves as the parameter  $\delta$  is varied. Since the target wave solution has no  $\theta$  dependence, we can obtain  $\omega_T$  for the 2D system by solving the 1D radial CGLE:

$$\begin{aligned} \partial_t A = & [1 + (\nu + i\delta)e^{-r^2/r_o^2}]A - (1 + i\alpha) \\ & \times |A|^2 A + (1 + i\beta) \left( \frac{\partial^2}{\partial r^2} + \frac{1}{r} \frac{\partial}{\partial r} \right) A. \end{aligned} \quad (6)$$

We use a split-step method, discretizing both space and time, and apply Neumann boundary conditions at  $r = 0$  and  $r = r_{max} = 100$ . The large  $r$  asymptotic wave number  $k$  is determined by a linear fit of the phase of  $A$  as a function of  $r$ . The frequency  $\omega_T$  is then given by the dispersion relation of Eq. (3). Initially we start with uniform initial conditions,  $|A(r, t = 0)| = \text{const}$  and the phase  $\phi(r, t = 0) = 0$ , and evolve the solution until the pattern is established. We then vary  $\delta$  in small steps  $\Delta\delta$ , keeping the other parameters fixed. As  $\delta$  is varied the final solution for the previous  $\delta$  is used as the initial condition for  $\delta + \Delta\delta$ . In this way we attempt to follow a particular branch of the solution (i.e., stationary targets or breathing targets) for as long as possible. We do this calculation for both increasing and decreasing  $\delta$ . The results are shown in Fig. 4. For  $\delta < 0.3$  the system undergoes a bulk oscillation, where the magnitude is constant in time and the phase far from the inhomogeneity is constant in space, but varying in time with a frequency of  $\alpha$ . That is,  $A = |A| \exp(-i\alpha t)$ , corresponding to  $k = 0$  in Eq. (2). Stationary target waves exist in the region of  $0.3 < \delta < 0.98$ , and

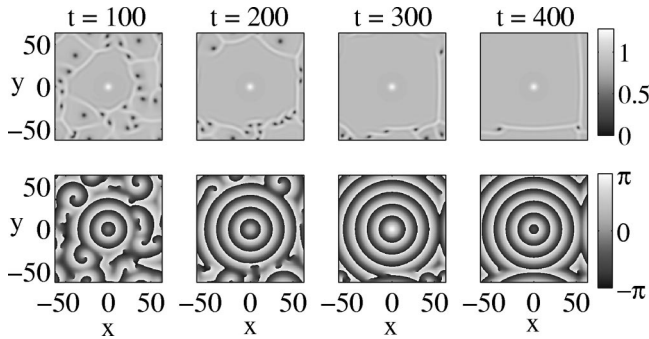


FIG. 7. Time evolution of both the magnitude (top) and phase (bottom) of  $A$  for  $\delta=0.7$ , where the stationary target dominates over spirals. This corresponds to region II in Fig. 4.

breathing target waves occur for  $\delta>0.8$ . Hysteresis between the stationary and breathing target waves is shown in Fig. 4 by the overlap region  $0.8<\delta<0.98$ .

As  $\delta$  is increased we observe that the stationary target branch [computed from the 1D CGLE, Eq. (6)] terminates at  $\delta=0.98$ . We interpret this as being due to a loss of stability of the radiated outward propagating waves. In particular, for our  $\alpha$  and  $\beta$  values, an *absolute instability* of the plane waves [19] occurs for  $\omega<-0.39$ , or equivalently  $|k|=0.639$  from the dispersion relation [Eq. (3)]. We thus expect that, as  $\omega_T$  approaches this range, the stationary target branch becomes unstable, and our solution of Eq. (6) will jump to the breathing target branch. That stability of the outward propagating waves is the relevant mechanism is supported by our 1D radial solutions for  $\delta$  near, but less than 0.98 (with Neumann boundary conditions at  $r=r_{max}=100$ ). These solutions show a spatially oscillatory behavior propagating inward from  $r_{max}$ , and decaying as it propagates toward  $r=0$ . As  $\delta$  draws nearer to 0.98 these oscillations become larger, and reach in to smaller  $r$  values, approaching  $r=0$  at  $\delta=0.98$ .

As  $\delta$  is decreased we observe that the breathing target branch [computed from the 1D CGLE (6)] terminates at  $\delta=0.8$ . To gain insight into the nature of this termination, refer to Figs. 5(a) and 5(b), which show the frequency  $\Omega$  and oscillation amplitude  $M_o$  of  $|A|$  at  $r=0$  as a function of  $\delta$ . As  $\delta$  approaches the critical value  $\delta=0.8$  from above, we note that neither  $\Omega$  or  $M_o$  approach zero. This is apparently consistent with the bifurcation that produces breathing tar-

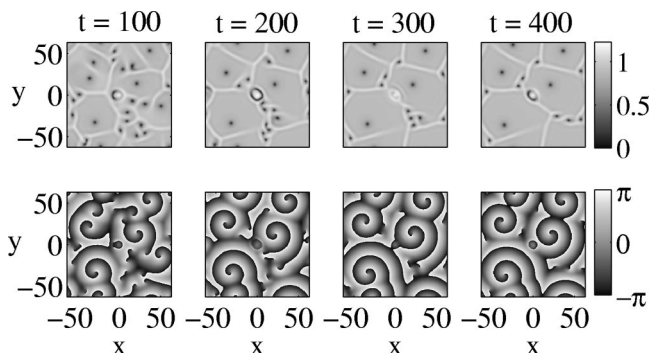


FIG. 8. Time evolution of both the magnitude (top) and phase (bottom) of  $A$  for  $\delta=1.5$ , where spirals dominate over the breathing target. This corresponds to region IV in Fig. 4.

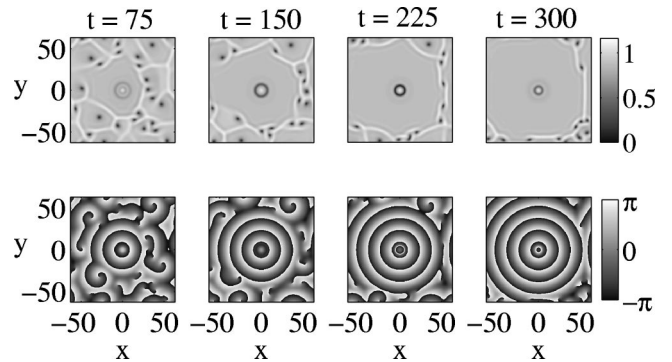


FIG. 9. Time evolution of both the magnitude (top) and phase (bottom) of  $A$  for  $\delta=3$ , where the breathing target dominates. This corresponds to region V in Fig. 4.

gets being a saddle-node bifurcation, but is inconsistent with it being either a Hopf bifurcation (which would have  $M_o=0$  at the critical  $\delta$ ) or a saddle connection bifurcation (which would have  $\Omega=0$  at the critical  $\delta$ ) [20].

### III. PATTERN COMPETITION

Several researchers reported on the competition between spatial patterns [10,18,21,22]. In our system there is competition between target and spiral waves. To study pattern competition we perform 2D numerical solutions of the CGLE with periodic boundary conditions and with a single inhomogeneity of the form of Eq. (5) placed in the middle of the simulation domain. For these numerical computations  $r_o$  is small compared to the periodicity length  $L(r_o/L=0.0318)$ .

The dominant pattern is predicted to be the pattern whose domain walls move outward, increasing the domain size at the expense of the adjacent competing domains. Requiring that the phase of the solution be continuous across domain boundaries provides an equation for the velocity of the domain walls [21], and this equation shows that, for the case when  $\beta<\alpha$ , as we have, the pattern with the lowest frequency dominates [23]. Figure 4 shows the frequency of target waves  $\omega_T$  versus  $\delta$  obtained from the 1D radial CGLE, [Eq. (6)], along with the spiral frequency  $\omega_s$  (horizontal line). Our prediction is that, if the system has a target frequency  $\omega_T$  higher than the spiral frequency  $\omega_s$ , then spiral waves will dominate; otherwise a target wave will dominate. To test this we perform two-dimensional numerical solutions of Eqs. (4) and (5) with periodic boundary conditions (as in Refs. [16–18,21]), and start with random initial conditions ( $A$  at each spatial point is randomly chosen from within the unit circle in the complex plane). There are different behaviors observed in five distinct regions of the parameter  $\delta$ . Region I has  $\delta<0.59$ , and spiral waves are the dominant pattern, since  $\omega_s<\omega_T$ . Figure 6 shows the time evolution for a system with  $\delta=0.5$  where there is competition between the spiral waves ( $\omega_s=0.08145$ ) and the stationary target waves ( $\omega_T=0.1574$ ). In region II,  $0.59<\delta<0.8$ , the stationary target wave dominates. An example is shown in Fig. 7, where  $\delta=0.7$ . Region III is the overlap region with  $0.8<\delta<0.97$ . In this hysteresis region, we observe that spiral waves or a stationary target wave can dominate. To which pattern the system goes is dependent on the initial conditions. The basin of attraction for the stationary target wave seems to become

smaller as  $\delta$  is increased. That is, if we start with initial conditions close to a stationary target wave, then the stationary target becomes the dominant pattern of the system since it has the lowest frequency. However, when we start with random initial conditions, we only see the stationary target wave solution when  $\delta$  is slightly larger than 0.8 (for example, see Fig. 2, which evolved from random initial conditions); otherwise the system goes to spiral waves. This sensitive dependence on the initial conditions probably results from the stationary target wave solution being near to the absolute instability. In region IV, where  $0.97 < \delta < 2.43$ ,  $\omega_s$  is less than  $\omega_T$  for the breathing target, and we obtain quasi-frozen spiral patterns as in region I. Figure 8 shows the spiral formation when  $\delta = 1.5$ . Finally, in region V, with  $\delta > 2.43$ ,  $\omega_T$  for the breathing target solution is less than  $\omega_s$ , and our

2D evolution from random initial conditions yields a breathing target wave; see Fig. 9, where  $\delta = 3$ .

#### IV. CONCLUSION

By introducing a localized inhomogeneity into the complex Ginzburg-Landau equation, we have been able to produce two different kinds of target waves: a stationary target wave, where  $|A|$  remains constant in time; and a breathing target wave, where  $|A|$  in the central region of the target oscillates periodically in time. Hysteresis is found to exist between these two solutions as the parameter  $\delta$  is varied. The theoretical prediction that the lower frequency pattern dominates (for  $\beta < \alpha$ ) describes well the competition between targets and spirals in our 2D numerical simulations.

- 
- [1] *Chemical Waves and Patterns*, edited by R. Kapral and K. Showalter (Kluwer Academic, Dordrecht, 1993).
- [2] M. Bär, A.K. Bangia, I.G. Kevrekidis, G. Haas, H.-H. Rotermund, and G. Ertl, *J. Phys. Chem.* **100**, 19 106 (1996).
- [3] A.J. Durston, *Diagn. Cytopathol* **37**, 225 (1974).
- [4] K.J. Lee, E.C. Cox, and R.E. Goldstein, *Phys. Rev. Lett.* **76**, 1174 (1996).
- [5] A.T. Winfree, *Chaos* **8**, 1 (1998) and references therein; F.X. Witkowski, L.J. Leon, P.A. Penkoske, W.R. Giles, M.L. Spano, W.L. Ditto, and A.T. Winfree, *Nature (London)* **392**, 78 (1998).
- [6] Y.A. Astrov, I. Müller, E. Ammelt, and H.-G. Purwins, *Phys. Rev. Lett.* **80**, 5341 (1998).
- [7] A.N. Zaikin and A.M. Zhabotinsky, *Nature (London)* **225**, 535 (1970).
- [8] A.T. Winfree, *Theor. Chem.* **4**, 1 (1978).
- [9] A.E. Bugrim, M. Dolnik, A.M. Zhabotinsky, and I.R. Epstein, *J. Phys. Chem.* **100**, 19 017 (1996).
- [10] K.J. Lee, *Phys. Rev. Lett.* **79**, 2907 (1997).
- [11] V. Petrov, Q. Ouyang, G. Li, and H.L. Swinney, *J. Phys. Chem.* **100**, 18 992 (1996).
- [12] P.S. Hagan, *Adv Appl. Math.* **2**, 400 (1981); N. Kopell, *ibid.* **2**, 389 (1981).
- [13] M.C. Cross and P.C. Hohenberg, *Rev. Mod. Phys.* **65**, 851 (1993); Y. Kuramoto, *Chemical Oscillations, Waves, and Turbulence* (Springer-Verlag, New York, 1984).
- [14] V.M. Eguiluz, E. Hernandez-Garcia, and O. Piro, *Int. J. Bifurcation Chaos Appl. Sci. Eng.* **9**, 2209 (1999).
- [15] P.S. Hagan, *SIAM (Soc. Ind. Appl. Math.) J. Appl. Math.* **42**, 762 (1982).
- [16] H. Chaté and P. Manneville, *Physica A* **224**, 348 (1996); G. Huber, P. Alström, and T. Bohr, *Phys. Rev. Lett.* **69**, 2380 (1992); I.S. Aranson, L. Aranson, L. Kramer, and A. Weber, *Phys. Rev. A* **46**, R2992 (1992).
- [17] T. Bohr, G. Huber, and E. Ott, *Physica D* **106**, 95 (1997).
- [18] M. Hendrey, E. Ott, and T.M. Antonsen, Jr., *Phys. Rev. Lett.* **82**, 859 (1999); *Phys. Rev. E* **61**, 4943 (2000).
- [19] I.S. Aranson, L. Aranson, L. Kramer, and A. Weber, *Phys. Rev. A* **46**, R2992 (1992). Absolute instability is defined to occur if a localized initial perturbation leads to subsequent perturbation growth at the  $(x,y)$  point at which the initial perturbation was introduced.
- [20] J. Guckenheimer and P. Holmes, *Nonlinear Oscillations, Dynamical Systems, and Bifurcations of Vector Fields* (Springer, New York, 1983). Due to the symmetry of the CGLE to the transformation  $A \rightarrow Ae^{i\phi}$ , in our consideration of the bifurcation of the breathing target, we consider it to be akin to a periodic orbit of a system without symmetry even though there are two incommensurate frequencies  $\omega_T$  and  $\Omega$  (note, however, that  $|A|$  varies periodically at  $\Omega$  with no  $\omega_T$  variation).
- [21] K. Nam, E. Ott, M. Gabbay, and P. Guzdar, *Physica D* **118**, 69 (1998).
- [22] I. Aranson, H. Levine, and L. Tsimring, *Phys. Rev. Lett.* **76**, 1170 (1996).
- [23] For  $\beta > \alpha$ , the pattern with the highest frequency dominates.